Theoretical Investigation of Competing Mechanisms in the Thermal Unimolecular Decomposition of Acetic Acid and the Hydration Reaction of Ketene

Xiaofeng Duan and Michael Page*

Contribution from the Department of Chemistry, North Dakota State University, Fargo, North Dakota 58105

Received October 12, 1994[⊗]

Abstract: We present ab initio multiconfiguration self consistent field calculations, using a polarized basis set, of equilibrium and transition-state structures relevant to the two competing mechanisms for the unimolecular decomposition of acetic acid. Single-point calculations using a modified Gaussian-2 method indicate that the lowest energy decomposition pathway for acetic acid is decarboxylation through a four-center transition state leading to methane and carbon dioxide, with a barrier of 71.8 kcal/mol. Dehydration, leading to ketene and water, has a calculated overall activation energy of 73.1 kcal/mol and occurs most easily through a two-step mechanism: 1,3 hydrogen migration to an enediol followed by elimination of water via a four-center transition state. The direct (one-step) dehydration of acetic acid has a calculated barrier of 76.4 kcal/mol. Transition state theory calculations indicate that all three decomposition routes are competitive at high temperatures: the predicted branching between decarboxylation, one-step dehydration, and two-step dehydration is 1.00:0.34:0.28 at 900 K and 1.00:1.11:0.31 at 1500 K. The hydration of ketene to acetic acid in the gas phase is predicted to occur competitively at high temperature by addition of water to the CO π-bond followed by a 1,3 hydrogen migration and by one-step addition to the CC π-bond.

I. Introduction

The gas-phase unimolecular decomposition of acetic acid occurs through two competing mechanisms: dehydration leading to water and ketene, and decarboxylation leading to methane and carbon dioxide.

$$CH_3COOH \rightarrow H_2O + CH_2CO \quad (1)$$

$$\rightarrow CH_4 + CO_2 \quad (2)$$

Bamford and Dewar[1] measured the activation energies for the dehydration and decarboxylation channels in a flow system at 1068−1218 K and found activation energies of 67.5 and 62.0 kcal/mol, respectively. Blake and Jackson studied this system in both batch and flow systems[2,3] and found, at temperatures above 1000 K where the decomposition was first order, an activation energy of 64.9 kcal/mol for the dehydration process. These authors consider that a possible contribution from a bimolecular mechanism may yield an artificially low activation energy for the unimolecular process and thus suggest that the 67.5 kcal/mol activation energy determined by Bamford and Dewar may be more realistic. The decarboxylation reaction was observed by Blake and Jackson to have an activation energy of 58.5 kcal/mol measured in a batch system and an activation energy of 69.8 kcal/mol measured in a flow system. Ruelle has speculated based on ab initio calculations that the smaller activation energy observed in the static system may result from a bimolecular decomposition mechanism where the decarboxyation is assisted by a water molecule generated in a previous unimolecular step. Mackie and Doolan[4] measured the decomposition of acetic acid in a shock tube at 1300−1950 K and concluded that the decomposition occurs via two competing unimolecular pathways (reactions 1 and 2) of about equal importance and both with activation energies of 72.7 kcal/mol. Thus measured activation energies for reaction 1 are in the range 67.5−72.7 kcal/mol, while measured activation energies for reaction 2 are about the same or somewhat lower and are in the range 64.9−72.7 kcal/mol.

Theoretical studies, by contrast, obtain activation energies for both channels that are considerably higher than experiment.[5−8] Furthermore, decarboxylation (reaction 2) is predicted to have an activation energy higher than that for dehydration. The most sophisticated calculations performed for the decarboxylation process (MP4/6-31G//HF/6-31G) obtain a reaction barrier of 89.3 kcal/mol,[5] a value 17 kcal/mol higher than the highest experimental determination of the activation energy. The most sophisticated calculations for the dehydration process[8] (MP4/6-31G*//HF/6-31G*) obtain an activation barrier of 81.3 kcal/mol for reaction 1 and an activation barrier of 80.6 kcal/mol for a two-step dehydration process: isomerization to an enediol via a 1,3 hydrogen transfer, followed by water elimination via a four-center transition state.

$$CH_3COOH \rightarrow CH_2C(OH)_2 \quad (3)$$

$$CH_2C(OH)_2 \rightarrow H_2O + CH_2CO \quad (4)$$

These calculated activation barriers are 8 kcal/mol higher than the highest experimental determination of the activation energies.

This paper reports calculations of the transition-state structures and activation energies for reactions 1−4 to investigate the competition between decarboxylation and dehydration in the unimolecular decomposition of acetic acid and the competition between the one-step (reaction 1) and the two-step (reactions 3

[⊗] Abstract published in *Advance ACS Abstracts*, April 1, 1995.

(1) Bamford, C. H.; Dewar, M. J. S. *J. Chem. Soc.* **1949**, 2877.
(2) Blake, P. G.; Jackson, G. E. *J. Chem. Soc. B* **1968**, 1153.
(3) Blake, P. G.; Jackson, G. E. *J. Chem. Soc. B* **1969**, 94.
(4) Mackie, J. C.; Doolan, K. R. *Int. J. Chem. Kinet.* **1984**, *16*, 525.
(5) Ruelle, P. *Chem. Phys.* **1986**, *110*, 263.
(6) Nguyen, M. T.; Ruelle, P. *Chem. Phys. Lett.* **1987**, *138*, 486.
(7) Xie, J. F.; Yu, J. G.; Feng, W. L.; Liu, R. Z. *J. Mol. Struct. (Theochem)* **1989**, *201*, 249.
(8) Skancke, P. N. *J. Phys. Chem.* **1992**, *96*, 8065.

0002-7863/95/1517-5114$09.00/0

Table 1. 10-in-10/6-31G* CASSCF and SCF Optimized Equilibrium Structures (Bond Lengths in Å and Bond Angles in deg)

	cis-acetic acid		*trans*-acetic acid		enediol		ketene	
parameter	CASSCF	SCF[a]	CASSCF	SCF[a]	CASSCF	SCF[b]	CASSCF	SCF[a]
C1−C2	1.527	1.501	1.537	1.501	1.348	1.320	1.332	1.305
C1−O1	1.193	1.187	1.188	1.181	1.374	1.345	1.162	1.145
C1−O2	1.370	1.331	1.377	1.337	1.351	1.334		
O2−H0	0.974	0.948	0.970	0.943	0.971			
O1−H1					0.967			
C2−H1	1.102	1.079	1.101	1.079			1.071	1.071
C2−H2	1.083	1.084	1.085	1.086	1.074		1.071	1.071
C2−H3	1.083	1.084	1.085	1.086	1.079			
C2−C1−O2	111.6	111.9	115.9	115.3	122.4	123.5	180.0	180.0
O1−C1−O2	122.5	122.4	119.6	120.5	110.8	110.3		
H0−O2−C1	105.9	108.3	109.2	112.4	106.7	109.4		
H1−O1−C1					109.9	110.6		
H1−C2−C1	108.9	109.6	108.7	109.3				
H2−C2−C1	109.7	109.6	110.3	110.3	121.2		119.4	119.2
H3−C2−C1	109.7	109.6	110.3	110.3	119.7		119.4	119.2
C2−C1−O2−O1	180.0	180.0	180.0	180.0	181.4			
H0−O2−C1−C2	180.0	180.0	0.0	0.0	156.0			
H1−O1−C1−C2					−6.0			
H1−C2−C1−O1	0.0	0.0	0.0	0.0			0.0	0.0
H2−C2−C1−O1	120.5	121.1	119.9	120.4	−2.7		180.0	180.0
H3−C2−C1−O1	−120.5	−121.1	−119.9	−120.4	181.5			

[a] With 6-31G** basis set, taken from ref 5. [b] With b-31G* basis set, taken from ref 8.

and 4) mechanisms for the dehydration reaction. These calculations are the first to consider the effects of electron correlation in the determination of the transition-state structures, the first to consider basis set effects on the relative energies beyond a single set of polarization functions, and the first to obtain results that are close to experimental measurements. Details of the ab initio electronic structure methods are presented in the next section. These are followed by a transition state theory treatment of the temperature dependence of the product branching based on the ab initio data.

II. Computational Methods

Geometry optimizations were performed with a complete active space self-consistent field (CASSCF) wave function[9,10] and a 6-31G* basis set.[11] The CASSCF wave function is a multiconfiguration SCF wave function that includes all configurations of a given spin multiplicity that can be constructed distributing a set of *active* electrons among a set of *active* orbitals. In the present calculations, the active space was designed to correlate all two-electron bonds that are severed in *any* of the reaction channels 1−4. In this way, the same active space is used for all reaction channels, and all reactant and transition-state structures are on a single potential energy surface. This leads to the correlation of five bonds, or an active space of 10 electrons distributed among 10 orbitals. The resulting 10-in-10 CASSCF wave function includes 19 404 singlet configurations. Reaction 1 requires the correlation of one CH bond, the CC bond, and the CO single bond of acetic acid. Reaction 2 requires in addition the correlation of the OH bond. Reaction 3 requires in addition correlation of the CO π-bond. Finally, all necessary bonds for reaction 4 are already correlated from consideration of reactions 1−3. Harmonic vibrational frequencies are determined analytically[12] at the CASSCF in 10-in-10/6-31G* level at all stationary points both to characterize properly the stationary point and to determine the corrections for zero-point vibrational energy. All MCSCF calculations were performed using the MESA[13] system of programs on four IBM RS/6000 computers dedicated to quantum chemistry calculations in the Chemistry Department at North Dakota State University.

Overall energetics were determined by single-point calculations using essentially the Gaussian-2 (G2) method described in detail elsewhere.[14] The two deviations between our calculations and the G2 method as described in ref 13 are (1) our use of geometries determined at the CASSCF 10-in-10/6-31G* level instead of the MP2/6-31G* level and (2) our use of zero-point vibrational energy corrections based on CASSCF 10-in-10/6-31G* frequencies instead of on scaled HF/6-31G* frequencies. All Moller−Plesset perturbation theory and quadratic CI calculations were performed with the Gaussian-92 program[15] on an IBM RS/6000(970) at North Dakota State University.

Generally, G2 is based on additive corrections to MP4/6-311G(d,p) energies, with consideration of diffuse basis functions on the second-row atoms, higher polarization functions (3d,f on second-row atoms and 2p on hydrogen atoms), and electron correlation beyond fourth order in perturbation theory through quadratic configuration interaction calculations. The G2 method also includes a higher level correction (HLC) that is based on the number of valence electron pairs. This number is, in principle, difficult to determine in transition-state regions of the potential energy surface where bonds are partially broken and formed and there may be partial biradical character. However, in the present calculations, examination of the occupation numbers of the MCSCF natural orbitals indicates the number of valence electron pairs remains essentially the same during the course of reactions 1−4. In particular, the lowest occupation number of the ostensibly doubly occupied orbitals in the equilibrium acetic acid structure is 1.98, while occupation numbers for the transition states never fall below 1.95. Therefore reported energy differences include no higher level corrections. Additionally, the fact that the molecular orbitals stay nearly doubly occupied during the course of reactions 1−4 justifies the use of the single-reference-configuration based methods in the G2 determination of the energetics.

III. Results and Discussion

a. Structures. Fully optimized structures are presented in Tables 1 and 2 for acetic acid with both cis and trans orientations

(9) Roos, B. O.; Taylor, P. R.; Siegbahn, P. E. M. *J. Chem. Phys.* **1980**, *48*, 157.

(10) Roos, B. O. In *Ab Initio Methods in Quantum Chemistry*; Lawley, K. P., Ed.; Wiley: New York, 1987; p 399.

(11) Hehre, W. J.; Radom, L.; Schleyer, P. v. R.; Pople, J. A. *Ab Initio Molecular Orbital Theory*; Wiley: New York, 1986.

(12) Page, M.; Saxe, P.; Adams, G. F.; Lengsfield, B. H. *J. Chem. Phys.* **1984**, *81*, 434.

(13) MESA (Molecular Electronic Structure Applications): Saxe, P.; Lengsfield, B. H.; Martin, R.; Page, M., copyright 1990, University of California.

(14) Curtiss, L. A.; Raghavachari, K.; Trucks, G. W.; Pople, J. A. *J. Chem. Phys.* **1991**, *94*, 7221.

(15) *Gaussian 92*, Revision A.; Frisch, M. A.; Trucks, G. W.; Head-Gordon, M.; Gill, P. M. W.; Wong, M. W.; Foresman, J. B.; Johnson, B. G.; Schlegel, H. B.; Robb, M. A.; Replogle, E. S.; Gomperts, R.; Andres, J. L.; Raghavachari, K.; Binkley, J. S.; Gonzalez, C.; Martin, R. L.; Fox, D. J.; Defrees, D. J.; Baker, J.; Stewart, J. J. P.; Pople, J. A. Gaussian Inc.: Pittsburgh, PA, 1992.

Table 2. 10-in-10/6-31G* CASSCF and SCF Optimized Transition-State Structures (Bond Lengths in Å and Bond Angles in deg)

	TS1		TS2		TS3		TS4	
parameter	CASSCF	SCF[a]	CASSCF	SCF[a]	CASSCF	SCF[b]	CASSCF	SCF[b]
C1–C2	1.452	1.439	1.937	1.967	1.443	1.431	1.344	1.316
C1–O1	1.142	1.122	1.160	1.150	1.293	1.260	1.603	1.530
C1–O2	1.874	1.998	1.268	1.239	1.302	1.296	1.262	1.259
O2–H0	0.978	0.945	1.303	1.228	0.972		1.352	1.346
O2–H1	1.204	1.252						
O1–H0							1.167	1.146
O1–H1					1.213	1.206	0.980	
C2–H0			1.390	1.405				
C2–H1	1.461	1.330	1.116	1.078	1.566	1.535		
C2–H2	1.083	1.082	1.079	1.087	1.082		1.070	
C2–H3	1.080	1.082	1.079	1.087	1.078		1.072	
C2–C1–O1	154.4	163.1	112.1	114.4	110.0	108.9		
C2–C1–O2	89.1	83.3	103.4	99.5	129.5		145.3	
O1–C1–O2	114.1		144.5		120.6		96.3	96.6
H0–O1–C1							70.0	72.8
H0–O2–C1	110.8		67.1	71.4	109.9			
H0–O2–H1	109.9	131.2						
H1–O1–C1					78.5		108.4	
H1–O2–C1	68.0	64.6						
H1–C2–C1	76.7	83.6	127.5	91.9	54.5	64.2		
H2–C2–C1	110.4	109.9	99.9	118.3	110.9		121.4	
H3–C2–C1	112.2	109.9	99.9	118.3	117.9		118.4	
C2–C1–O2–O1	190.9		180.0		186.9		179.9	
C2–C1–O2–H1	11.4	0.4						
H0–O2–H1–C2	91.5	133.1						
H0–O2–C1–O1							−0.8	2.4
H0–O2–C1–C2	92.5		0.0	0.0	193.3			
H1–C2–C1–O1					9.07	9.5	26.6	
H1–C2–C1–O2	8.9		0.0					
H2–C2–C1–O1	118.5	60.0	57.5	111.7	74.4		1.7	
H3–C2–C1–O1	−8.3	−60.0	−57.5	−111.7	−153.2		179.8	

[a] With 6-31G** basis set, taken from ref 5. [b] With 6-31G* basis set, taken from ref 8.

of the COOH group, the enediol intermediate, ketene, and four transition states corresponding to reactions 1–4 and numbered accordingly. These represent the first calculated structures for acetic acid and the transition-state species that include the effects of electron correlation. Hartree–Fock structures are included in the tables for comparison.

The cis and trans conformers of acetic acid should be reasonably well described at the Hartree–Fock level. Indeed, the only significant differences involve the five bonds being correlated. As is usually the case, the inclusion of valence correlation effects lengthens these bonds. The CO π-bond is lengthened by 0.007 Å, while the CC, CO, OH, and CH σ-bonds are lengthened by 0.0036, 0.040, 0.027, and 0.022 Å, respectively.

Not surprisingly, electron correlation has a more significant effect on the structures of the transition states. The significant differences are found for bonds being broken and formed in the reactions. The transition state for the one-step dehydration process (reaction 1) is shown in Figure 2 and is denoted TS1. Here the breaking CH bond is 0.012 Å *shorter* at the HF level, while the incipient OH bond is 0.06 Å *longer* at the HF level. Put another way, in the MCSCF transition state, the breaking CH bond is stretched 34% beyond its equilibrium value, and the forming OH bond is stretched by 24% beyond its equilibrium value. Thus, this transition state is shifted a little toward products, as is expected for a reacion that is 34 kcal/mol endothermic. For the Hartree–Fock structure, however, the CH bond is stretched by only 24%, while the forming OH bond is stretched by 36% beyond its equilibrium value. Additionally, the breaking CO bond is 0.094 Å longer at the Hartree–Fock level. Indeed, Skancke[8] noted for the reverse of this reaction (addition of water across the CC double bond) that based on the Hartree–Fock transition-state structure, the CH bond largely

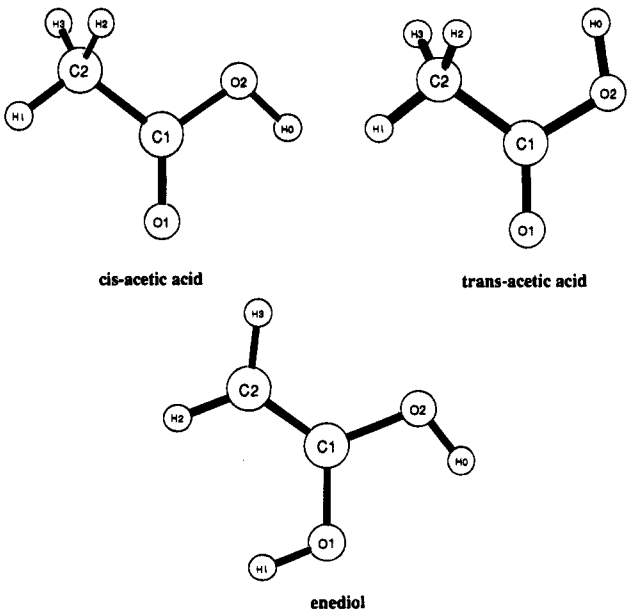

Figure 1. CASSCF 10-in-10/6-31G* structures of *cis*- and *trans*-acetic acid and the lowest energy conformer of the isomeric enediol. Structural parameters are listed in Table 1.

formed before the CO bond formed. He thus suggested that the reaction could be viewed as electrophilic attack on the β-carbon of ketene. Examination of the MCSCF structure in Figure 2, however, reveals that the two bonds are largely formed simultaneously. At the transition state, the CH and CO bonds are 34 and 36% beyond their equilibrium values.

Similarly large descrepencies can be found for the other transition states as well. For TS2, the decarboxylation reaction,

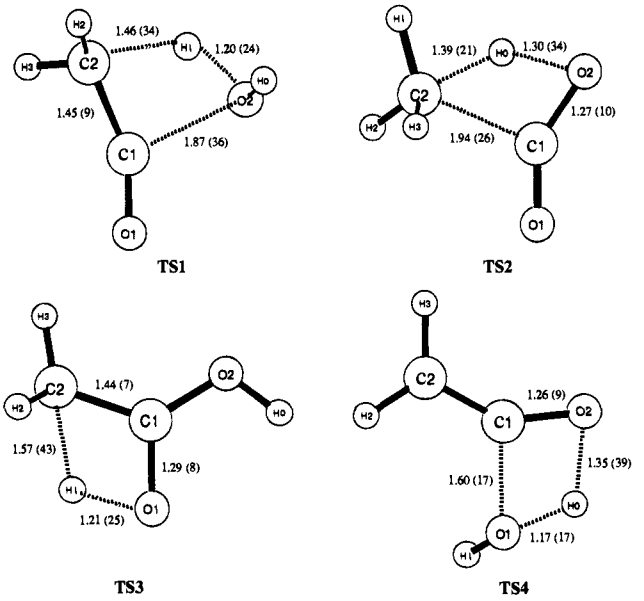

Figure 2. CASSCF 10-in-10/6-31G* optimized transition structures for the direct dehydration reaction of acetic acid (TS1), the decarboxylation reaction of acetic acid (TS2), the 1,3 hydrogen migration from acetic acid to the enediol (TS3), and the dehydration reaction from the enediol (TS4). Selected bond lengths are given in angstroms. Percent extension from equilibrium bond lengths is given in parentheses. Complete structural parameters are listed in Table 2.

the Hartree–Fock values for the breaking CC and OH bonds are 0.112 Å longer and 0.068 Å shorter than the MCSCF values, respectively. It is interesting to note that while the correlation effects on the transition-state structures are substantial, analysis of the MCSCF wave function indicates that multiconfigurational effects do not play a significant role in the electronic structure. The geometry is simply sensitive to these relatively small effects.

The CASSCF/6-31G* vibrational frequencies and resulting zero-point vibrational energies are listed in Table 3 for *cis*- and *trans*-acetic acid, the enediol, and the four transition states. Zero-point vibrational energies are determined from the unscaled frequencies.

b. Energetics. Relative energies calculated at the CASSCF 10-in-10 geometries and using the modified G2 technique as described earlier are shown and compared with previous calculations in Table 4 and are displayed in Figure 3. Ruelle performed single-point Moller–Plesset fourth-order perturbation theory (MP4) calculations using a 6-31G basis set at structures calculated at the Hartree–Fock (HF) level with a 6-31G basis set. These calculations are denoted MP4/6-31G//HF/6-31G. At this level of theory, the dehydration process has an activation barrier of 78.4 kcal/mol, and the decarboxylation process has an activation barrier of 89.3 kcal/mol. Although these are the highest level calculations performed by Ruelle on the acetic acid system, he speculates based on higher level calculations for the formic acid system that structure reoptimization at the MP2 level would lower the dehydration barrier by 1.6 kcal/mol, and that polarization functions in the basis set along with structures calculated at the MP2 level would lower the decarboxylation barrier by 12 kcal/mol. In a subsequent paper, Nguyen and Ruelle point out that both transition-state structures considered by Ruelle in ref 5 are actually second-order saddle points. If Reulle's structures were optimized at the same level of theory as the energetics were determined, then the second-order saddle points would guarantee the existence of lower energy first-order saddle points. However, because the energetics were determined by performing single-point calculations at a higher level of theory, no such claim could be made.

Xie et al.[7] obtained an activation barrier for reaction 2 of 86.0 kcal/mol at the MP4(without triple excitations)/3-21G//HF/3-21G level. They also report an activation barrier at the same level for dehydration via the two-step mechanism of 83.0 kcal/mol, with the higher barrier occurring for reaction 3.

Skancke[8] was the first to perform energy calculations using a polarized basis set for any of reactions 1–4 and was the first to use a polarized basis set for the geometry optimizations. Skancke's focus was on the hydration reaction of ketene, for which he considered four possibilities: addition of both monomeric and dimeric H_2O to both the CO and CC double bonds of ketene. The dimeric addition reactions were both found to have activation barriers considerably lower than those for monomeric addition. Skancke's calculated activation barriers for the monomeric addition of water to ketene agree quite well with the present calculations. His calculated energies for the first and second steps for the monomeric addition to the CO double bond (relative to water plus ketene) are 39.7 and 40.3 kcal/mol, compared to the present energies of 38.2 and 38.7 kcal/mol for these same steps. Skancke computed the barrier for addition to the CC double bond to be 41.0 kcal/mol, only 0.7 kcal/mol higher than the second step of the two-step addition

Table 3. 10-in-10/6-31G* CASSCF Harmonic Vibrational Frequencies (cm^{-1}) and Zero-Point Energies (kcal/mol)

	acetic acid							
	cis	trans	enediol	ketene	TS1	TS2	TS3	TS4
ν_1	107.6	139.7	199.8	406.2	1993.2i	2455.1i	2326.6i	1919.8i
ν_2	416.3	335.3	337.6	507.0	231.9	223.5	391.1	396.2
ν_3	515.3	426.6	468.1	686.1	313.4	336.5	501.4	417.9
ν_4	595.1	563.9	541.7	1055.6	440.1	510.0	563.0	587.0
ν_5	604.4	611.1	622.4	1174.6	548.3	560.1	658.8	619.1
ν_6	863.7	859.9	757.1	1563.4	615.6	638.5	780.4	682.2
ν_7	1050.0	1042.2	842.0	2270.7	750.2	754.2	907.5	769.3
ν_8	1120.5	1111.3	941.3	3368.4	801.2	843.7	1020.7	799.5
ν_9	1263.6	1267.6	1049.0	3472.4	894.1	1183.1	1165.7	1065.1
ν_{10}	1427.0	1384.1	1277.0		1028.5	1305.2	1252.0	1083.9
ν_{11}	1516.0	1506.9	1320.3		1179.2	1387.0	1296.4	1223.6
ν_{12}	1570.8	1578.2	1491.5		1558.9	1535.0	1542.4	1492.3
ν_{13}	1606.8	1608.4	1574.4		1664.6	1563.9	1623.5	1574.3
ν_{14}	1994.0	2012.9	1818.0		1866.9	1906.9	1637.5	1890.7
ν_{15}	3073.3	3081.4	3317.1		2208.8	2179.4	2102.1	2197.7
ν_{16}	3262.2	3240.3	3414.7		3260.8	2933.8	3269.8	3369.3
ν_{17}	3300.9	3278.1	3751.8		3343.1	3298.0	3356.3	3469.1
ν_{18}	3728.5	3767.8	3792.4		3703.1	3375.4	3733.0	3684.9
ZPE	40.05	39.77	39.34	20.73	34.89	35.07	36.89	36.20

Table 4. Calculated Activation Energies for Dehydration and Decarboxylation Reactions of Acetic Acid (Energies in kcal/mol Relative to Acetic Acid and Corrected for Zero-Point Vibrational Energy Differences)

investigator (ref)	geometry method	energy method	activation energy
	Dehydration		
one step			
Ruelle (5)	HF/6-31G	MP4/6-31G	78.4
Skancke (8)	HF/6-31G*	MP4/6-31G*	81.3
this work	MCSCF[a]/6-31G*	G2	76.4
two steps			
Xie et al. (7)	HF/3-21G	MP4(SDQ)/3-21G	83.0
Skancke (8)	HF/6-31G*	MP4/6-31G*	80.6
this work	MCSCF[a]/6-31G*	G2	73.1
experiment (see text)	67.5−72.7		
	decarboxylation		
Ruelle (5)	HF/6-31G	MP4/6-31G	89.3
Xie et al. (7)	HF/3-21G	MP4(SDQ)/3-21G	86.0
this work	MCSCF[a]/6-31G*	G2	71.8
experiment (see text)			62.0−72.6

[a] Complete active space SCF distributing 10 electrons among 10 orbitals.

process. Our activation barrier for addition to the CC double bond is 42.0 kcal/mol, which is 3.3 kcal/mol higher than the second step of the two-step addition process.

The lowest energy decomposition route for acetic acid, as shown in Figure 3, is decarboxylation yielding methane and carbon dioxide. Our calculated activation barrier for this process, 71.8 kcal/mol, is much lower than previous calculations (89.3[5] and 86.0[7] kcal/mol), is consistent with the measured activation energies of Mackie and Doolan[4] (72.6 kcal/mol) and Blake and Jackson[2,3] (69.8 kcal/mol), and is higher than the early determination of Bamford and Dewar[1] (62.0 kcal/mol).

For the dehydration process, our calculations predict the lowest energy route to be 1,3 hydrogen migration yielding an enediol with an activation barrier of 73.1 kcal/mol, followed by a four-center elimination of water with an activation barrier of 72.6 kcal/mol (relative to acetic acid). The direct elimination of water from acetic acid has an activation barrier of 76.4 kcal/mol, 3.3 kcal/mol higher than the two-step process. Once again, our calculated activation barrier for dehydration of 73.1 kcal/mol is considerably lower than previous theoretical determinations and is in the vicinity of Mackie and Doolan's experimental activation energy of 72.7 kcal/mol.[4]

c. Thermal Decomposition. In determining the branching between the two products channels, we consider that the $H_2O + CH_2CO$ products can be reached directly, via TS1, or indirectly, via isomerization to the enediol intermediate (TS3) followed by four-center elimination (TS4). The kinetic scheme is shown below, where the subscripts on the rate constants refer to the labeling of the transition structures in Figure 3.

$$CH_3COOH \underset{k_{-3}}{\overset{k_3}{\rightleftharpoons}} CH_2C(OH)_2 \xrightarrow{k_4} CH_2CO + H_2O$$

$$\xrightarrow{k_1} CH_2CO + H_2O$$

$$\xrightarrow{k_2} CH_4 + CO_2$$

A steady-state treatment on the enediol intermediate yields the following expressions for the observed rate coefficients

$$k(H_2O) = k_1 + \frac{k_3}{1 + k_{-3}/k_4}$$

$$k(CO_2) = k_2$$

The CASSCF 10-in-10 structures, the harmonic vibrational frequencies, and the energetics determined with the modified G2 method can be used to determine transition state theory estimates of the rate constants for thermal decomposition in the high-pressure limit. In computing the partition functions, all internal modes were treated as harmonic oscillators with the

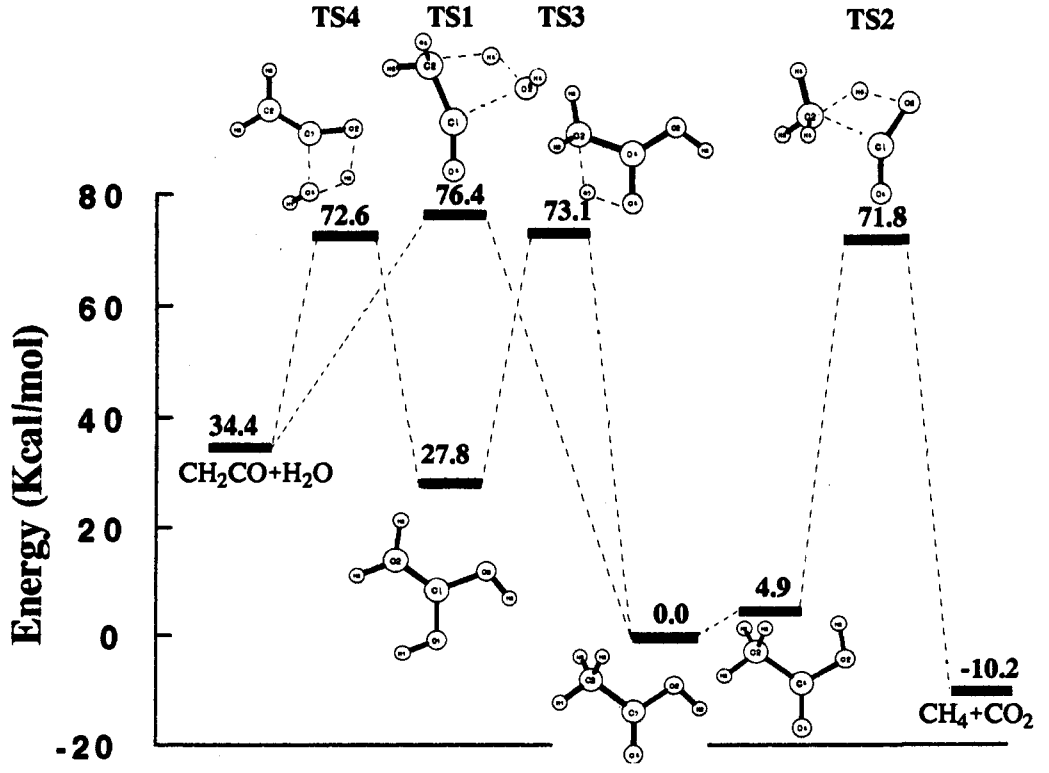

Figure 3. Relative enthalpies (at 0 K) for competing decomposition pathways for acetic acid. Single-point energies are determined using the Gaussian-2 method at structures optimized at the CASSCF 10-in-10/6-31G* level.

exception of the nearly free methyl rotation in the acetic acid reactant. This degree of freedom, closely represented by the normal mode with harmonic frequency of 107.6 cm^{-1} (see Table 3), was treated as a free rotor with a reduced moment of inertia[16] of 2.91 amu $Å^2$ and an internal-rotation symmetry number of 3. The OH torsion in acetic acid was treated as a vibration because it has a much higher harmonic vibrational frequency of 515 cm^{-1} and has an internal rotation barrier somewhat greater than 5 kcal/mol (the energy of the trans isomer). The reaction path degeneracy is three for TS1 and TS3 (elimination of methyl hydrogen) and one for TS2 (elimination of hydroxyl hydrogen).

The transition state theory treatment gives the following Arrhenius parameters (kcal/mol) at 1000 K:

$$k(CO_2) = k_2 = 10^{13.85} \exp(-74.6/RT)$$

$$k_1 = 10^{14.65} \exp(-79.8/RT)$$

$$k_3 = 10^{13.55} \exp(-75.0/RT)$$

$$k_{-3}/k_4 = 10^{-0.38} \exp(+0.09/RT)$$

The analysis above leads to the following observed Arrhenius parameters for water elimination determined at 1000 K,

$$k(H_2O) = 10^{14.47} \exp(-78.0/RT)$$

Mackie and Doolan[4] report activation energies of 72.6 ± 3.6 and 72.7 ± 3.6 kcal/mol for water and carbon dioxide production, respectively, with identical preexponential factors ($\log A = 13.1 \pm 0.3$ s^{-1}) for the two channels. The calculated activation energy for CO_2 production, 74.6 kcal/mol, is in good agreement with this experimental determination, while the calculated activation energy for H_2O production, 78.0 kcal/mol, is 1.8 kcal/mol above Mackie's and Doolan's reported uncertainty. However, because the calculations predict a larger preexponential factor for H_2O production than for CO_2 production, the calculated and measured branching ratios are qualitatively similar, and the overall predicted rate constants are within a factor of 2 at 1000 K. The above calculations predict $[CO_2]/[H_2O] = 1.6$ at 900 K, 1.0 at 1200 K, and 0.7 at 1500 K. Mackie and Doolan predict a branching ratio ($[CO_2]/[H_2O]$) of about unity at 1300 K.[4] Saito, Sasaki, Yoshinobu, and Imamura,[17] in their shock tube study of the decomposition of ethyl acetate, also report a branching ratio for secondary acetic acid decomposition of around unity in this same temperature range.

Our calculations also predict that the direct and two-step mechanisms for water production are competitive with one another. In particular, at 900 K 55% of the $H_2O + CH_2CO$ comes from the direct, one-step mechanism, whereas at 1500 K 78% comes from the direct mechanism. There are two reasons our calculations predict a larger preexponential factor for H_2O production than for CO_2 production: TS1 leading to $H_2O + CH_2CO$ is somewhat looser than TS2 leading to $CO_2 + CH_4$, as can be seen from the vibrational frequencies in Table 3; and the reaction path degeneracy of 3 for decomposition via TS1 increases the preexponential factor by $\log(3.0) = 0.48$.

A similar analysis can be applied to the hydrolosis of ketene. The transition state theory calculations predict that addition of water to the CO π-bond of ketene is competitive with addition to the CC π-bond, accounting for 67% of the reaction at 1000 K and 48% of the reaction at 1500 K. For the acetic acid produced via hydrolosis of ketene, the steady-state treatment of the enediol intermediate reduces the above percentages to 38% and 22% at 1000 and 1500 K, respectively, that is, at 1000 K 38% of the acetic acid produced by reaction of water with ketene proceeds via addition of water to the CO π-bond of ketene followed by a 1,3 hydrogen shift.

IV. Summary

We present ab initio multiconfiguration self consistent field calculations, using a polarized basis set, of equilibrium and transition-state structures relevant to competing mechanisms for the unimolecular decomposition of acetic acid. By comparison with previous calculations at the Hartree−Fock level with the same basis set, it is shown that the transition-state structures are significantly affected by electron correlation. Single-point calculations using a modified Gaussian-2 method indicate that the lowest energy decomposition pathway for acetic acid is decarboxylation through a four-center transition state leading to methane and carbon dioxide, with a barrier of 71.8 kcal/mol. Dehydration, leading to ketene and water, has a calculated overall activation energy of 73.1 kcal/mol and occurs most easily through a two-step mechanism: 1,3 hydrogen migration to an enediol followed by elimination of water via a four-center transition state. The direct (one-step) dehydration of acetic acid has a calculated barrier of 76.4 kcal/mol. The hydration of ketene to acetic acid in the gas phase is predicted to occur more readily by addition of water to the CO π-bond rather than the CC π-bond.

Transition state theory calculations indicate that all three decomposition routes are competitive at high temperatures: the predicted branching between decarboxylation, one-step dehydration, and two-step dehydration is 1.00:0.34:0.28 at 900 K and 1.00:1.11:0.31 at 1500 K. The hydration of ketene to acetic acid in the gas phase is predicted to occur competitively at high temperature by addition of water to the CO π-bond followed by a 1,3 hydrogen migration and by one-step addition to the CC π-bond.

JA943339S

(16) Herzberg, G. *Infrared and Raman Spectra of Polyatomic Molecules*; Van Nostrand Reinhold Co.: New York, 1945; p 511.

(17) Saito, K.; Sasaki, T.; Yoshinobu, I.; Imamura, A. *Chem. Phys. Lett.* **1990**, *170*, 385.